Volume 11
Number 6
14 February 2020
Pages 1443–1716

Chemical Science

rsc.li/chemical-science

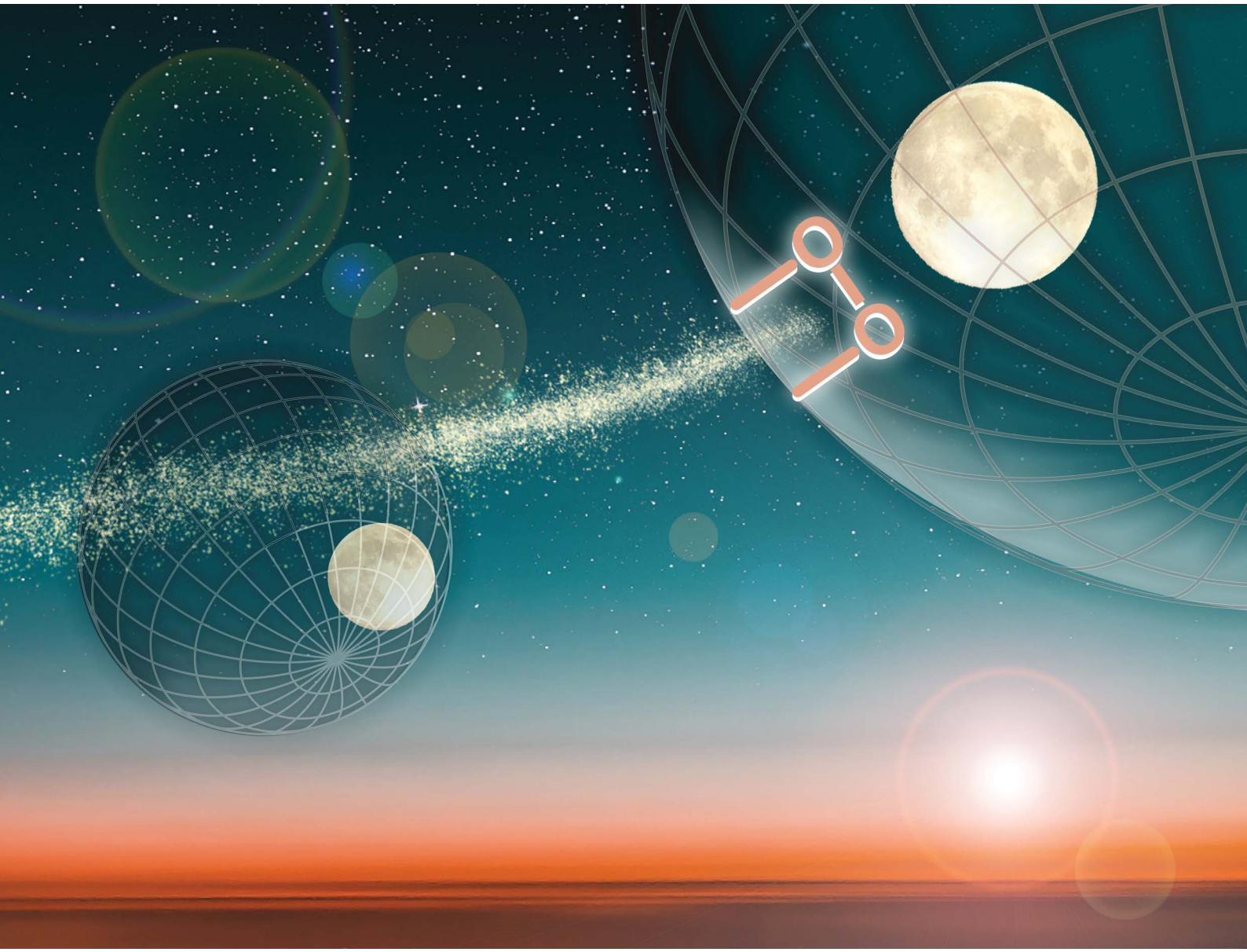

ISSN 2041-6539

ROYAL SOCIETY OF CHEMISTRY

EDGE ARTICLE
Dario M. Bassani, Brigitte Bibal *et al.*
Singlet oxygen stimulus for switchable functional organic cages

Chemical Science

ROYAL SOCIETY OF CHEMISTRY

EDGE ARTICLE

View Article Online
View Journal | View Issue

Cite this: *Chem. Sci.*, 2020, **11**, 1478

All publication charges for this article have been paid for by the Royal Society of Chemistry

Singlet oxygen stimulus for switchable functional organic cages†‡

Cédric Mongin, §¶ Alejandro Mendez Ardoy,¶ Raphaël Méreau, Dario M. Bassani * and Brigitte Bibal *

Molecular cages **1a** and **2a** incorporating a 9,10-diphenylanthracene (DPA) chromophore were synthesized through a templated ring-closure metathesis approach that allows variation in cavity size through the introduction of up to three different pillars. Reversible Diels–Alder reaction between the DPA moiety and photogenerated singlet oxygen smoothly converted **1a** and **2a** to the corresponding endoperoxide cages **1b** and **2b**, which are converted back to **1a** and **2a** upon heating. Endoperoxide formation constitutes a reversible covalent signal that combines structural changes in the interior of the cage with introduction of two additional coordination sites. This results in a large modulation of the binding ability of the receptors attributed to a change in the location of the preferred binding site owing to the added coordination by the endoperoxide oxygen lone pairs. Cages **1a** and **2a** form complexes with sodium and cesium whose association constants are modified by 4–20 fold for Na^+ and 200–450 fold for Cs^+ upon conversion to **1b** and **2b**. DFT calculations show that in the anthracene form, cages **1a** and **2a** can bind 2 metal cations in their periphery so that each cation is coordinated by 4 oxygens and one amine nitrogen, whereas the endoperoxide cages **1b** and **2b** bind cations centrally in a geometry that favors coordination to the endoperoxide oxygens.

Received 24th October 2019
Accepted 15th January 2020

DOI: 10.1039/c9sc05354a

rsc.li/chemical-science

Introduction

Molecular cages represent a versatile class of molecules that recognize and bind guests within a confined space defined by the structural parameters imposed by their molecular constituents.[1–3] Compared to open or flexible receptors, they exhibit unique abilities for selective guest sequestration, sensing, transport (drug delivery) or transformation (nanoreactor, catalyst).[4]

Recently, switchable metallocages emerged as attractive nano-objects able to tune on demand their chemical structures and therefore their binding abilities.[5,6] The reversible changes within hosts then allow an *in situ* modulation of guest binding constant,[5b] with some examples of guest catch-and-release.[5a,5d,6a,6c] This emerging area aims to implement reversibility in molecular sequestration to further advances in catalysis as well as biomedical and environmental applications.

Currently, the stimuli-response metallocages rely on known switches based on photo-reactions[5] or redox reactions[6] under light/heat or electrochemical control. To extend the possibilities of adjustable cages, we envisioned that the molecular reversible [4π + 2π] reaction between anthracene and singlet oxygen could be a new switch available under smooth conditions with potential biomedical applications.[7] In addition, we proposed that the covalently modified organic cage can benefit from the temporary presence of the endoperoxide functional group as an additional *endo* binding site. To the best of our knowledge, no example of the use of endoperoxides as a recognition feature has been reported.

In comparison to metallocages whose efficient preparation exploits self-assembly by directed coordination but limits the functionalization of the cavity, organic cages require multi-step synthesis but can be decorated with various *endo* functional groups. With regards to switchable covalent organic containers, only two studies by Houk and co-workers described hemicarcerands possessing reversibly open *versus* closed pillars.[8] These systems exploited reversible disulfide/thiol formation or the dimerization of anthracenes as switches for encapsulation of benzene derivatives by size complementarity. Nonetheless, despite significant progress benefitting from the development of click and dynamic covalent chemistry,[9] the synthetic access to organic covalent cages and the modulation of their structure

Université de Bordeaux, CNRS, Bordeaux INP, ISM UMR 5255, 351 cours de la Libération, 33400 Talence, France. E-mail: dario.bassani@u-bordeaux.fr; brigitte.bibal@u-bordeaux.fr

† Dedicated to Professor Jean-Marie Lehn on the occasion of his 80th birthday.

‡ Electronic supplementary information (ESI) available: Experimental procedures, (host : guest) titrations, spectral and crystallographic data, modelling. CCDC 1541525 and 1541528. For ESI and crystallographic data in CIF or other electronic format see DOI: 10.1039/c9sc05354a

§ Present address: Laboratoire PPSM – CNRS UMR 8531, ENS Paris-Saclay, 61 avenue du Président Wilson, 94230 Cachan, France.

¶ These authors contributed equally to this work.

and properties using an external stimulus remains a significant challenge.

Herein, we explore the reversible addition of singlet oxygen to 9,10-diphenylanthracene (DPA) as a molecular switch for the reversible tuning of the binding properties of a molecular cage. In particular, we aim to tune the guest localization within a polytopic cage depending on its switch state. Diphenylanthracene is well known for its ability to smoothly react with singlet oxygen ($^1O_2$) to form stable 9,10-endoperoxides whose thermal cycloreversion is also highly efficient and affords the parent anthracene chromophore.[7,10] The process involves the [4π + 2π] reaction in which light is used to *in situ* generate $^1O_2$ through energy transfer from ^{3}(DPA)* or through the use of an external photosensitizer. To date, this reversible reaction on DPA was mainly employed for the sensing or delivery of $^1O_2$ with a few reports of fatigue over several cycles.[11,12]

Although anthracene-based receptors and containers[13] exist (some of which exploit the reversible dimerization of anthracenes),[14] there has been no investigation of the use of the $^1O_2$ addition/cycloreversion reaction to reversibly tune their binding properties, except for the pseudo-rotaxane developed by Smith[15] for a near-infrared dye catch-and-release system. To this end, cages **1a** and **2a** were designed to incorporate a DPA unit and two podand pillars for the complexation of metallic cations (Fig. 1). The sequential reactivity of cyanuric chloride towards substitution is used to incorporate two different lengths of the polyether chain ($n = 2$, 4). The corresponding endoperoxides **1b** and **2b** exploit a photo-triggered molecular change in structure and coordination number that significantly modifies their allosteric binding properties.

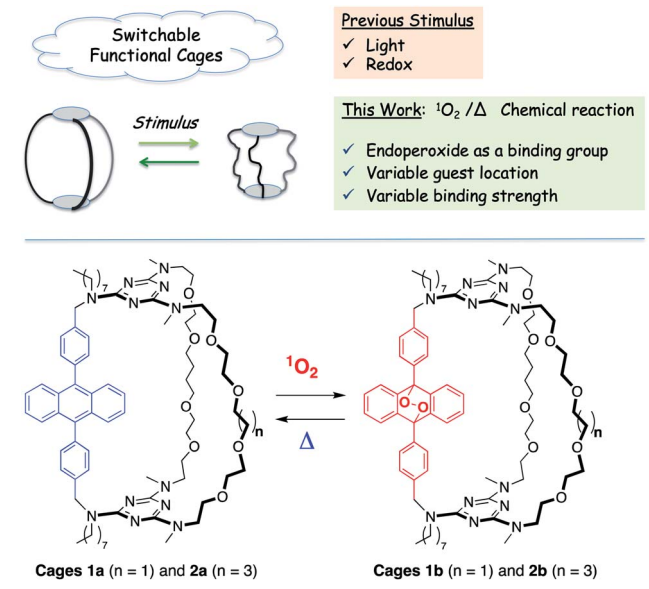

Fig. 1 Concept of switchable functional cages in which structural modification upon stimulus leads to binding variations. Previously, photo- and redox reactions were described whereas this work presents a $^1O_2$ stimulated cage that allows changes in guest localization and binding strength within host due to an endoperoxide formation. The structures of cages **1** and **2**, that differ by the length of one pillar.

Results and discussion

Synthesis and characterization of switchable DPA cages

The synthetic pathway selected to prepare DPA-based containers incorporating three (**1a**) or two (**2a**) different pillars (Schemes 1 and 2). It relies on the selective sequential aromatic nucleophilic substitution of cyanuric chloride by different amine nucleophiles.[16] Cation-templated ring-closure metathesis (RCM) adapted from the "magic ring" method[17] was chosen to perform the final macrocyclization. Reports of molecular containers prepared using RCM are relatively scarce, with some examples employing hydrogen-bonds[18] or coordination chemistry[19] to template ring closure. Hydrogenation of the double bonds then affords the desired organic cages containing three pillars.

Both containers **1a** and **2a** were prepared from diamine **3**. The synthesis of **1a** (Scheme 1) relies on the one-pot formation of macrocycle **6** through two successive substitutions of cyanuric chloride by **3** at 20 °C, then diamine **5** at 40 °C (60% overall yield). Attempts to achieve the third macrocyclisation using a third diamine failed, resulting in oligomerization and insoluble products. Therefore, the final macrocyclization was undertaken according to the strategy described in Scheme 1. Substitution of the two triazine moieties in **6** by monoamine **7** at 90 °C led to bis-allyl compound **8** (92% yield). Ring-closing metathesis (95% yield) in the presence of NaBArF (1 equiv., BArF = tetrakis(3,5-bis(trifluoromethyl)phenyl)borate) followed by hydrogenation of the olefin (99% yield) allowed the isolation of pure container **1a**. In the absence of sodium cations, oligomerization of the bis-allyl macrocycle was instead observed.

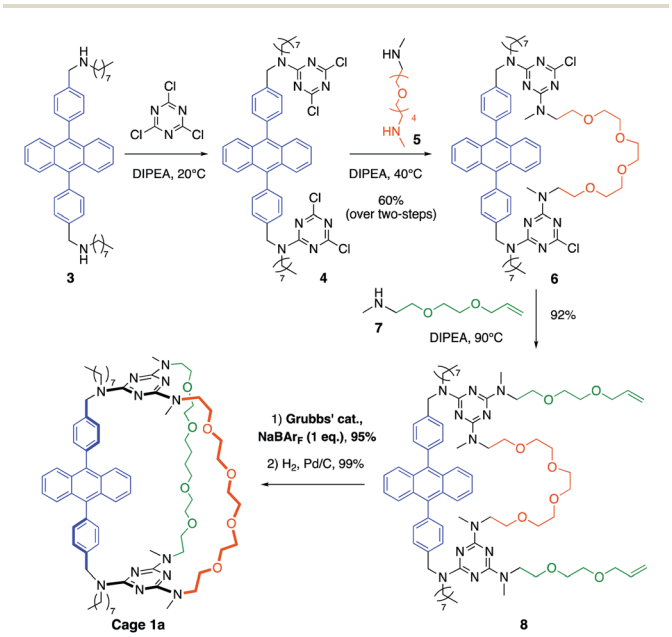

Scheme 1 Synthetic strategy used to prepare organic cages with three different pillars, illustrated with cage **1a**. The three first steps exploit the sequential tri-substitution of cyanuric chloride at different temperatures and the final ring-closure is a templated metathesis.

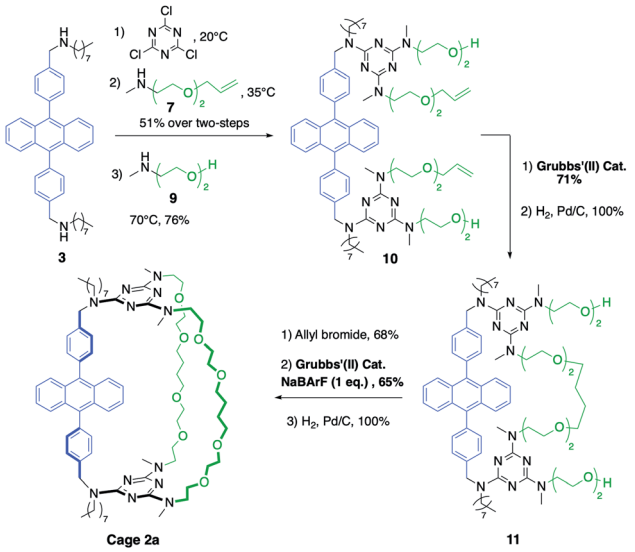

Scheme 2 Synthesis of cage **2a** containing two kind of pillars, obtained through two successive ring-closure metatheses.

The larger cage **2a** was synthesized through two successive ring-closure metatheses to form a symmetric pseudo crown-ether (Scheme 2). In a one-pot reaction, cyanuric chloride (2 equiv.) underwent two successive substitutions, first by diamine **3** at 20 °C, followed by monoamine **7** at 35 °C (51% overall yield). The third substitution on each triazine moiety was achieved with amino-alcohol **9** at 70 °C (76% yield) to afford compound **10**. The first RCM was successfully achieved without the use of NaBArF as template in 71% yield and it was followed by a quantitative hydrogenation to give macrocycle **11**. Finally, two allyl groups were introduced on the alcohol substituents (68% yield) and a second RCM, templated by NaBArF (1 equiv., 65% yield) provided compound **2a** after hydrogenation.

After purification by column chromatography, both cages **1a** and **2a** were isolated as cage compounds without any traces of oligomeric or dimeric macrocycles which are potential side-products from a divergent ring-closure metathesis, that was prevented by the controlled use of NaBArF as an efficient template (see ESI‡). Although single crystals suitable for crystallographic analysis could not be obtained, the structures and composition of **1a** and **2a** were confirmed by mass spectrometry and VT-NMR studies. At 20 °C, the NMR signals of **1a** and **2a** are complicated by significant signal broadening attributed to the presence of rotamers originating from the restricted rotation around the C(s-triazine)–*N*-(2,4,6-amino substituents) bonds[20] and to the different polyether conformers.

^{1}H VT-NMR (toluene-d_8, 293–373 K) allowed clear identification of the two cages by showing sharp signals for the polyether structure of the two pillars and the typical signature of DPA at higher temperatures. The absorption and emission properties of **1a** and **2a** ($\varepsilon_{max,\ 378\ nm} = 12\ 100\ M^{-1}\ cm^{-1}$, $\Phi_F = 0.95$, $\tau = 6.0$ ns in degassed dichloromethane) are similar to those of the parent DPA chromophore and show no appreciable solvatochromic behavior.[21]

Slow conversion of **1a** and **2a** to the corresponding endoperoxides **1b** and **2b** could be achieved by direct irradiation in O_2-saturated dichloromethane solutions, but this was found to be much faster when using a triplet photosensitizer such as methylene blue to generate $^1O_2$ (Fig. 2a). The use of a high boiling point solvent (propylene carbonate, 15 mol% methylene blue) allowed repeated interconversion between the DPA and endoperoxide forms by visible-light irradiation at 20 °C (2 h) to form **1b** and **2b**, followed by heating (140 °C, 1 h) to revert to **1a** and **2a**, respectively (Fig. 2b). Under these conditions, a fatigue of ≤10% is observed, possibly due to the oxidation side-products from anthracene that can occur during cycloreversion or resulting from the limited solubility of the compounds in propylene carbonate.[7,22]

Tunable binding properties of cages

The polyether chains in cages **1a** and **2a** are conducive to the binding of alkali metal cations.[23] Preliminary studies were conducted in dichloromethane solution using soluble cations of different ionic radius, *i.e.* NaBArF (*ca.* 1.0 Å) and CsBArF (*ca.* 1.7 Å) to evaluate the (host : guest) complementary by monitoring the fluorescence emission of the DPA chromophore. In the case of **1a**, the addition of Na^+ induced an initial decrease in fluorescence emission until 1 : 1 stoichiometry, followed by an increase in emission intensity to reach a value that is close to that of free **1a** in deaerated solutions at a 1 : 2 stoichiometry (Fig. 3a, red curve). Instead, binding of Cs^+ resulted in a monotonic decrease of the fluorescence emission consistent with a 1 : 1 stoichiometry (Fig. 3b, red curve). Non-linear least-squares fitting of the binding isotherms to a 1 : 2 or a 1 : 1 model for Na^+ or Cs^+ respectively, allowed the extraction of the

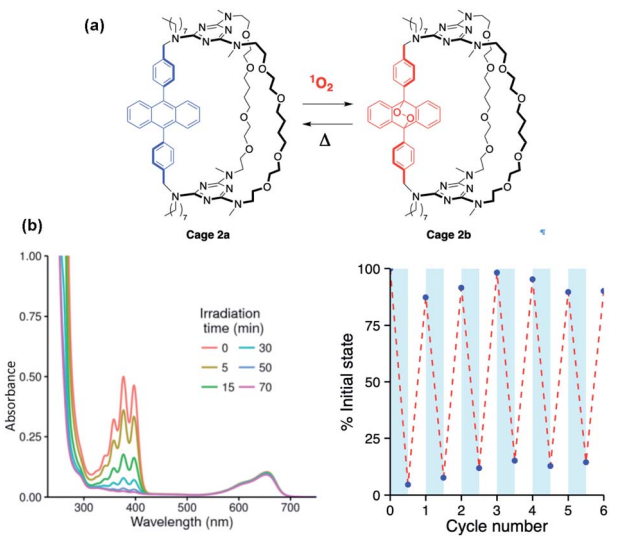

Fig. 2 Reversible transformation between cages **2a** and **2b** monitored by absorption spectroscopy: (a) formation of cage **2b** upon visible light irradiation of cage **2a** (40 μM in propylene carbonate containing 1.5 μM methylene blue). (b) Fatigue cycles for the **2a**/**2b** conversion in propylene carbonate in the presence of methylene blue as a photosensitizer. Cycloreversion is conducted by heating to 120 °C for 80–120 min.

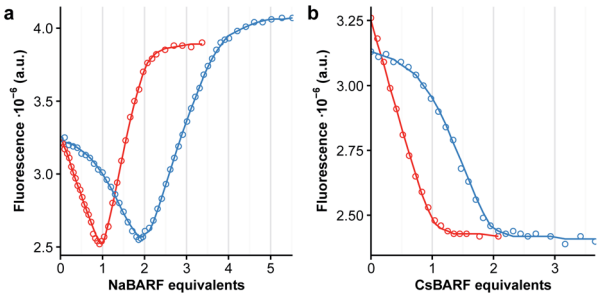

Fig. 3 Variation in fluorescence intensity (λ_{exc} = 365 nm, λ_{em} = 423 nm) of cage **1a** (red circles) in dichloromethane (15 μM) upon addition of NaBArF (panel a) or CsBArF (panel b). Red line represents best fit to a 1 : 2 (Na^+) or a 1 : 1 (Cs^+) binding isotherm using non-linear least-squares fitting. The data represented by the blue circles is obtained in the presence of 1 equiv. of **1b** in competitive binding assays.

binding constants for each cation. These are tabulated in Table 1, and evidence the very strong interactions between the cages and alkali metal ions (10–13 kcal mol^{-1}). Similar results were obtained with **2a**, with the exception that a weaker 1 : 2 complex with Cs^+ could also be detected. Compared to **1a**, the longer pillar in **2a** results in a larger binding cavity that better accommodates both 1 : 1 and 1 : 2 complexes, resulting in a *ca.* 100- and 400-fold increase in the observed association constants for Na^+ and Cs^+, respectively.

In the case of the non-emissive endoperoxide cages **1b** and **2b**, an indirect fluorescence titration method was employed using cages **1a** and **2a** as competitive fluorescent indicators. The addition of one equiv. of **1b** to a solution of **1a** results in a shift of the binding isotherms for both Na^+ and Cs^+ as shown in Fig. 3 (blue curves), indicating that the binding of the cages is enhanced upon endoperoxide formation. Fitting of the binding isotherms using the previously determined values for the binding of **1a** and **2a** allows the determination of the association constants for endoperoxides **1b** and **2b** (Table 1). In the case of **1**, formation of the endoperoxide results in the enhancement of the binding of the first Na^+, but not of the second cation, and in a *ca.* 20-fold increase in the binding of Cs^+. The situation is similar for **2**, with the exception that the larger cage accommodates better the presence of two Na^+ cations in the endoperoxide form. The somewhat lower binding of Cs^+ by **2b** *vs.* **2a** is instead unexpected and counter to the general trend observed.

Table 1 Binding constants (K, M^{-1})[a,b] between cages **1**–**2** and selected cations in dichloromethane

	Na^+		Cs^+	
	K_{11}	K_{12}	K_{11}	K_{12}
1a	6×10^8	3×10^6	1×10^7	—
1b	4×10^9	2×10^6	2×10^8	—
2a	1×10^{11}	2×10^8	4×10^9	3.3×10^6
2b	9×10^{12}	1×10^9	2×10^7	[c]

[a] Estimated errors: ±15%. [b] Host : guest stoichiometry is (1 : 1) or (1 : 2). [c] $<3 \times 10^6$.

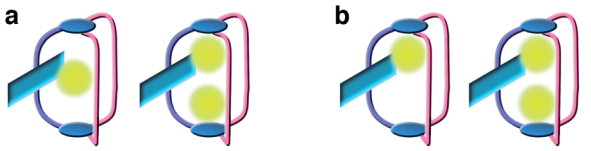

Fig. 4 Two possible binding sequences for the formation of a 1 : 1 and a 1 : 2 complex between **1** or **2** and Na^+. In (a), the first cation is bound near the DPA chromophore and undergoes translation upon binding of the second cation whereas in (b) two separate distal binding sites are sequentially occupied.

Binding of the first metal cation in **1** or **2** defines two possible binding models (Fig. 4) as it may take place near the anthracene ring (a), where it could benefit from π–cation interactions and vicinal ether coordination, or near the triazine moieties (b). In the first case, we may expect that binding of the second cation induces a translation of the first ion to the opposite end of the cage to accommodate the second cation and reduce coulombic repulsion.

Modelling

To further understand the binding of Na^+ and Cs^+ in **1** and **2**, possible 1 : 1 and 1 : 2 complexes were modeled using the Def2svp basis set[24] in DFT B3LYP[25] calculations to locate energy minima on the potential energy surface. The energies of these minima were then determined with greater precision using single point energy calculations at the post HF MP2(full)/Def2svp level. All calculations (geometry optimizations and single point energy) were performed using a polarizable continuum model to simulate solvent (see ESI‡ for details). The lowest energy structures found for Na^+ and Cs^+ complexes of **2a** and **2b** are shown in Fig. 5 (see ESI‡ for details).

The results show that, for the anthracene cages **1a** and **2a**, binding in the central position (Fig. 4a) is less favored than

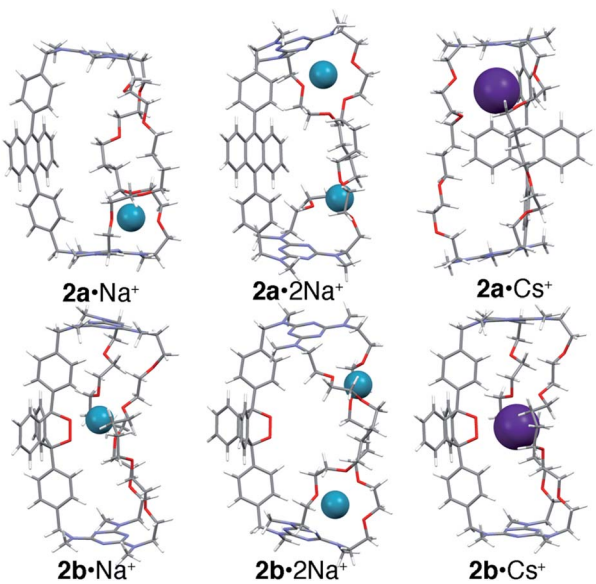

Fig. 5 Energy minimized structures of **2a** or **2b** with Na^+ (1 : 1 or 1 : 2) or Cs^+ (1 : 1).

binding vicinal to the triazines (Fig. 4b), where coordination of the metal cation by the ether linkages and one of the amine lone pairs is possible. Interestingly, binding of the first cation induces a significant conformational change that disrupts the coordination geometry at the second site, in agreement with the pronounced negative cooperativity observed experimentally.

In the case of the endoperoxide cages **1b** and **2b**, the preferred binding site is instead located near the endoperoxide site, where up to five oxygens can be coordinated (O–M^+ distances ≤ sum of the van der Waals radii). This is consistent with the 10-fold greater anticooperativity observed in binding the second cation in **1b** *vs.* **1a** and in **2b** *vs.* **2a** ($M^+ = Na^+$) since displacement of the first cation entails a loss in coordination by the endoperoxide oxygens. The calculations also show that binding of Cs^+ by **1** is significantly more favored when in the endoperoxide form **1b** than by the anthracene form **1a**. This, however, is not the case for cage **2** where the calculated difference in energy is instead very small. The reason for this becomes apparent upon closer inspection of the structures, which evidences that the tetramethylene segments in **1** and **2** are too long to allow optimal coordination of the centrally bound ion. This leads to the adoption of a *gga* conformation in **1b**·Cs^+, where the central *gauche* conformation has a C–C torsional angle of 80°. In the case of **2b**, the two tetramethylene segments adopt *gga* and *ggg* conformations with torsional angles for the central C–C bond of 69° and 89°, respectively. Therefore, despite the fact that both **1b** and **2b** bind Cs^+ through the formation of five coordination bonds to nearby oxygen atoms, the torsional strain required to achieve this is greater in **2b** *vs.* **1b**. In contrast, both **1a** and **2a** bind Cs^+ near one of the triazines nitrogens (d = 3.2 Å) within a pseudo-crown ether cavity formed by four ether oxygens.

In light of the computational results described above, the fluorescence quenching behavior observed upon complexation of Na^+ is intriguing. Quenching of emission in anthracene-containing organometallic complexes has been previously attributed to energy transfer from the excited anthracene chromophore to the ligated metal ion.[26] However, we may discount such processes in **1a**·Na^+ and **2a**·Na^+ on the basis that unlike transition metal ions, sodium ions do not possess low-lying excited states. Similar energetic considerations rule out quenching by electron transfer, and collisional quenching would be expected to be similarly efficient for both ions in the case of sequential binding of the cations in the vicinity of the triazines (Fig. 4b). To solve this conundrum, we surmised that the low polarity of dichloromethane might favor the formation of relatively tight ion pairs, and that the quenching might in fact result from the proximity of the BArF counterion. To test this, we proceeded to examine the bimolecular Stern–Volmer quenching of 9,10-diphenylanthracene in THF by NaBArF, which evidenced moderately efficient quenching with a bimolecular quenching rate of $k = 8.6 \times 10^8$ M^{-1} s^{-1} (see ESI‡). This suggests that ion pairing may indeed contribute to fluorescence quenching in host–guest complexes.

Conclusions

The covalent addition of singlet oxygen as reversible signal combines three distinct inputs: a structural change in the interior of the cage ($Csp^2 \rightarrow Csp^3$), loss of anthracene aromaticity, and introduction of two oxygen atoms capable of providing new coordinating sites. This results in a large modulation of the binding ability of the receptors and also, according to molecular modeling studies, a change in the location of the preferred binding site owing to the added coordination by the endoperoxide oxygen lone pairs. The inside volume of the cages is well suited for binding first-row alkali metal cations, including Cs^+ which is of interest as it is a common byproduct of nuclear fission.

Beyond the synthetic challenge of incorporating reversible covalent functionality in molecular receptors, the comparison of cages **1** and **2** also demonstrates how small geometrical variations in just one of three pillars may affect the binding ability and mechanism. This was possible thanks to the sequential substitution reactions in cyanuric chloride, which represents a valuable strategy for developing asymmetrical cages incorporating additional functionalities.

Conflicts of interest

There are no conflicts to declare.

Acknowledgements

The University of Bordeaux and CNRS are thanked for their support. Marion Tisseraud and Camille Bakkali Hassani are acknowledged for their contribution in the synthesis of precursors.

Notes and references

1 For a selection of reviews about metallocages, see: (*a*) M. Yoshizawa, J. K. Klosterman and M. Fujita, *Angew. Chem., Int. Ed.*, 2009, **48**, 3418–3438; (*b*) R. Chakrabarty, P. S. Mukherjee and P. J. Stang, *Chem. Rev.*, 2011, **111**, 6810–6918; (*c*) S. Durot, J. Taesch and V. Heitz, *Chem. Rev.*, 2014, **114**, 8542–8578; (*d*) M. Han, D. M. Engelhard and G. H. Clever, *Chem. Soc. Rev.*, 2014, **43**, 1848–1860; (*e*) M. Frank, M. D. Johnstone and G. H. Clever, *Chem.–Eur. J.*, 2016, **22**, 14104–14125; (*f*) S. Chakraborty and G. R. Newkome, *Chem. Soc. Rev.*, 2018, **47**, 3991–4016; (*g*) C.-Y. Zhu, M. Pan and C.-Y. Su, *Isr. J. Chem.*, 2019, **59**, 209–219; (*h*) M. Pan, J.-H. Zhang and C.-Y. Su, *Coord. Chem. Rev.*, 2019, **378**, 333–349; (*i*) L. Zhao, X. Jing, X. Li, X. Guo, L. Zeng, C. He and C. Duan, *Coord. Chem. Rev.*, 2019, **378**, 157–187.

2 For reviews about organic capsules, see: (*a*) L. R. MacGillivray and J. L. Atwood, *Angew. Chem., Int. Ed.*, 1999, **38**, 1018–1033; (*b*) J. Rebek Jr, *Angew. Chem., Int. Ed.*, 2005, **44**, 2068–2078; (*c*) S. Liu and B. C. Gibb, *Chem. Commun.*, 2008, 3709–3716; (*d*) L. Adriaenssens and P. Ballester, *Chem. Soc. Rev.*, 2013, **42**, 3261–3277; (*e*) J. H. Jordan and B. C. Gibb, *Chem. Soc. Rev.*,

2015, **44**, 547–585; (*f*) V. Ramamurthy, *Acc. Chem. Res.*, 2015, **48**, 2904–2917; (*g*) L. Catti, Q. Zhang and K. Tiefenbacher, *Chem.–Eur. J.*, 2016, **22**, 9060–9066; (*h*) L.-J. Chen, H.-B. Yang and M. Shionoya, *Chem. Soc. Rev.*, 2017, **46**, 2555–2576.

3 For recent reviews about organic cages, see: (*a*) G. Zhang and M. Mastalerz, *Chem. Soc. Rev.*, 2014, **43**, 1934–1947; (*b*) D. Zhang, A. Martinez and J.-P. Dutasta, *Chem. Rev.*, 2017, **117**, 4900–4942; (*c*) F. Beuerle and B. Gole, *Angew. Chem., Int. Ed.*, 2018, **57**, 4850–4878.

4 For recent reviews about functional cages, see: (*a*) A. Galan and P. Ballester, *Chem. Soc. Rev.*, 2016, **45**, 1720–1737; (*b*) C. Gropp, B. L. Quigley and F. Diederich, *J. Am. Chem. Soc.*, 2018, **140**, 2705–2717; (*c*) F. J. Rizzuto, L. K. S. von Krbek and J. R. Nitschke, *Nat. Rev. Chem.*, 2019, **3**, 204–222; (*d*) C. Tan, D. Chu, X. Tang, Y. Liu, W. Xuan and Y. Cui, *Chem.–Eur. J.*, 2019, **25**, 662–672; (*e*) L. L. K. Taylor, I. A. Riddell and M. M. J. Smulders, *Angew. Chem., Int. Ed.*, 2019, **58**, 1280–1307.

5 (*a*) T. Murase, S. Sato and M. Fujita, *Angew. Chem., Int. Ed.*, 2007, **46**, 5133–5136; (*b*) M. Han, R. Michel, B. He, Y.-S. Chen, D. Stalke, M. John and G. H. Clever, *Angew. Chem., Int. Ed.*, 2013, **52**, 1319–1323; (*c*) M. Han, Y. Luo, B. Damaschke, L. Gomez, X. Ribas, A. Jose, P. Peretzki, M. Seibt and G. H. Clever, *Angew. Chem., Int. Ed.*, 2016, **55**, 445–449; (*d*) R.-J. Li, J. J. Holstein, W. G. Hiller, J. Andréasson and G. H. Clever, *J. Am. Chem. Soc.*, 2019, **141**, 2097–2103.

6 (*a*) V. Croué, S. Goeb, G. Szaloki, M. Allain and M. Sallé, *Angew. Chem., Int. Ed.*, 2016, **55**, 1746–1750; (*b*) C. Colomban, G. Szaloki, M. Allain, L. Gomez, S. Goeb, M. Sallé, M. Costas and X. Ribas, *Chem.–Eur. J.*, 2017, **23**, 3016–3022; (*c*) G. Szaloki, V. Croué, V. Carré, F. Aubriet, O. Alévêque, E. Levillain, M. Allain, J. Arago, E. Orti, S. Goeb and M. Sallé, *Angew. Chem., Int. Ed.*, 2017, **56**, 16272–16276.

7 (*a*) N. J. Turro, M.-F. Chow and J. Rigaudy, *J. Am. Chem. Soc.*, 1979, **101**, 1300–1302; (*b*) N. J. Turro, M.-F. Chow and J. Rigaudy, *J. Am. Chem. Soc.*, 1981, **103**, 7218–7224; (*c*) J.-M. Aubry, C. Pierlot, J. Rigaudy and R. Schmidt, *Acc. Chem. Res.*, 2003, **36**, 668–675.

8 (*a*) R. C. Helgeson, A. E. Hayden and K. N. Houk, *J. Org. Chem.*, 2010, **75**, 570–575; (*b*) H. Wang, F. Liu, R. C. Helgeson and K. N. Houk, *Angew. Chem., Int. Ed.*, 2013, **52**, 655–659.

9 For recent examples, see: (*a*) B. J. Benke, P. Aich, Y. Kim, K. L. Kim, M. R. Rohman, S. Hong, I.-C. Hwang, E. H. Lee, J. H. Roh and K. Kim, *J. Am. Chem. Soc.*, 2017, **139**, 7432–7435; (*b*) L. A. Wessjohann, O. Kreye and D. G. Rivera, *Angew. Chem., Int. Ed.*, 2017, **56**, 3501–3505; (*c*) H. Qu, Y. Wang, Z. Li, X. Wang, H. Fang, Z. Tian and X. Cao, *J. Am. Chem. Soc.*, 2017, **139**, 18142–18145; (*d*) K. Ono, S. Shimo, K. Takahashi, H. Uekusa and N. Iwasawa, *Angew. Chem., Int. Ed.*, 2018, **57**, 3113–3117; (*e*) C. C. Pattillo and J. S. Moore, *Chem. Sci.*, 2019, **10**, 7043–7048; (*f*) M. Kolodziejski, A. R. Stefankiewicz and J.-M. Lehn, *Chem. Sci.*, 2019, **10**, 1836–1843; (*g*) T. H. G. Schick, J. C. Lauer, F. Rominger and M. Mastalerz, *Angew. Chem., Int. Ed.*, 2019, **58**, 1768–1773; (*h*) C. Bravin, A. Guidetti, G. Licini and C. Zonta, *Chem. Sci.*, 2019, **10**, 3523–3528.

10 (*a*) S. Miyamoto, G. R. Martinez, M. H. G. Medeiros and P. Di Mascio, *J. Am. Chem. Soc.*, 2003, **125**, 6172–6179; (*b*) W. Fudickar and T. Linker, *J. Am. Chem. Soc.*, 2012, **134**, 15071–15082.

11 (*a*) X. Li, G. Zhang, H. Ma, D. Zhang and D. Zhu, *J. Am. Chem. Soc.*, 2004, **126**, 11543–11548; (*b*) W. Fudickar, A. Fery and T. Linker, *J. Am. Chem. Soc.*, 2005, **127**, 9386–9387; (*c*) B. Song, G. Wang and J. Yuan, *Chem. Commun.*, 2005, 3553–3555; (*d*) S. Kim, T. Tachikawa, M. Fujitsuka and T. Majima, *J. Am. Chem. Soc.*, 2014, **136**, 11707–11715; (*e*) K. Liu, R. A. Lalancette and F. Jäkle, *J. Am. Chem. Soc.*, 2017, **139**, 18170–18173; (*f*) Y. Zhou, H.-Y. Zhang, Z.-Y. Zhang and Y. Liu, *J. Am. Chem. Soc.*, 2017, **139**, 7168–7171; (*g*) W.-L. Shan, W.-X. Gao, Y.-J. Lin and G.-X. Jin, *Dalton Trans.*, 2018, **47**, 2769–2777; (*h*) K. Liu, R. A. Lalancette and F. Jäkle, *J. Am. Chem. Soc.*, 2019, **141**, 7453–7462.

12 (*a*) A. M. Asadirad, Z. Erno and N. R. Branda, *Chem. Commun.*, 2013, **49**, 5639–5641; (*b*) S. Martins, J. P. S. Farinha, C. Baleizao and M. N. Berberan-Santos, *Chem. Commun.*, 2014, **50**, 3317–3320; (*c*) W. Fudickar and T. Linker, *Angew. Chem., Int. Ed.*, 2018, **57**, 12971–12975.

13 (*a*) F. Fages, J.-P. Desvergne, H. Bouas-Laurent, P. Marsau, J.-M. Lehn, F. Kotzyba-Hibert, A.-M. Albrecht-Gary and M. Al-Joubbeh, *J. Am. Chem. Soc.*, 1989, **111**, 8672–8680; (*b*) L. Fabbrizzi, I. Faravelli, G. Francese, M. Licchelli, A. Perotti and A. Taglietti, *Chem. Commun.*, 1998, 971–972; (*c*) M. Yoshizawa and J. K. Klosterman, *Chem. Soc. Rev.*, 2014, **43**, 1885–1898; (*d*) M. Yoshizawa and M. Yamashina, *Chem. Lett.*, 2017, **46**, 163–171; (*e*) K. Yazaki, M. Akita, S. Prusty, D. K. Chand, T. Kikuchi, H. Sato and M. Yoshizawa, *Nat. Commun.*, 2017, **8**, 15914.

14 (*a*) Y. Molard, D. M. Bassani, J.-P. Desvergne, P. N. Horton, M. B. Hursthouse and J. H. R. Tucker, *Angew. Chem., Int. Ed.*, 2005, **44**, 1072–1075; (*b*) C. Schäfer, R. Eckel, R. Ros, J. Mattay and D. J. Anselmetti, *J. Am. Chem. Soc.*, 2007, **129**, 1488–1489.

15 (*a*) J. M. Baumes, I. Murgu, A. Oliver and B. D. Smith, *Org. Lett.*, 2010, **12**, 4980–4983; (*b*) J. M. Baumes, J. J. Gassensmith, J. Giblin, J.-J. Lee, A. G. White, W. J. Culligan, W. M. Leevy, M. Kuno and B. D. Smith, *Nat. Chem.*, 2010, **2**, 1025–1030; (*c*) G. T. Spence, S. S. Lo, C. Ke, H. Destecroix, A. P. Davis, G. V. Hartland and B. D. Smith, *Chem.–Eur. J.*, 2014, **20**, 12628–12635.

16 (*a*) G. Blotny, *Tetrahedron*, 2006, **62**, 9507–9522; (*b*) *Chemistry of Heterocyclic compounds: s-triazines and derivatives*, ed. E. M. Smolin and L. Rapoport, John Wiley & Sons, 2008.

17 (*a*) C. Dietrich-Buchecker, G. Rapenne and J.-P. Sauvage, *Coord. Chem. Rev.*, 1999, **185–186**, 167–176; (*b*) T. J. Kidd, D. A. Leigh and A. J. Wilson, *J. Am. Chem. Soc.*, 1999, **121**, 1599–1600; (*c*) J. A. Wisner, P. D. Beer, M. G. Drew and M. R. Sambrook, *J. Am. Chem. Soc.*, 2002, **124**, 12469–12476; (*d*) A. F. M. Kilbinger, S. J. Cantrill, A. W. Waltman,

M. W. Day and R. H. Grubbs, *Angew. Chem., Int. Ed.*, 2003, **42**, 3281–3285.

18 (*a*) T. D. Clark and M. R. Ghadiri, *J. Am. Chem. Soc.*, 1995, **117**, 12364–12365; (*b*) O. Molokanova, A. Bogdan, M. O. Vysotsky, M. Bolte, T. Okai, Y. Okamoto and V. Böhmer, *Chem.–Eur. J.*, 2007, **13**, 6157–6170.

19 (*a*) T. Inomata and K. Konishi, *Chem. Commun.*, 2003, 1282–1283; (*b*) J. Taesch, V. Heitz, F. Topic and K. Rissanen, *Chem. Commun.*, 2012, **48**, 5118–5120; (*c*) B. Zhu, H. Chen, W. Lin, Y. Ye, J. Wu and S. Li, *J. Am. Chem. Soc.*, 2014, **136**, 15126–15129.

20 (*a*) M. Amm, N. Platzer, J. Guilhem, J.-P. Bouchet and J.-P. Volland, *Magn. Reson. Chem.*, 1998, **36**, 587–596; (*b*) H. E. Birkett, R. K. Harris, P. Hodgkinson, K. Carr, M. H. Charlton, J. C. Cherryman, A. M. Chippendale and R. P. Glover, *Magn. Reson. Chem.*, 2000, **38**, 504–511; (*c*) M. Fazekas, M. Pintea, P. Lameiras, A. Lesur, C. Berghian, I. Silaghi-Dumitrescu, N. Plé and M. Darabantu, *Eur. J. Org. Chem.*, 2008, 2473–2494.

21 (*a*) J. V. Morris, M. A. Mahaney and J. R. Huber, *J. Phys. Chem.*, 1976, **80**, 969–974; (*b*) S. Hamai and F. Hirayama, *J. Phys. Chem.*, 1983, **87**, 83–89; (*c*) S. R. Meech and D. J. Phillips, *J. Photochem.*, 1983, **23**, 193–217.

22 J. Rigaudy, P. Scribe and C. Brelière, *Tetrahedron*, 1981, **37**, 2585–2593.

23 G. W. Gokel, W. M. Leevy and M. E. Weber, *Chem. Rev.*, 2004, **104**, 2723–2750.

24 (*a*) F. Weigend and R. Ahlrichs, *Phys. Chem. Chem. Phys.*, 2005, **7**, 3297–3305; (*b*) F. Weigend, *Phys. Chem. Chem. Phys.*, 2006, **8**, 1057–1065.

25 (*a*) A. D. J. Becke, *Chem. Phys.*, 1993, **98**, 5648–5652; (*b*) C. Lee, W. Yang and R. G. Parr, *Phys. Rev. B: Condens. Matter Mater. Phys.*, 1988, **37**, 785–789; (*c*) S. H. Vosko, L. Wilk and M. Nusair, *Can. J. Phys.*, 1980, **58**, 1200–1211; (*d*) P. J. Stephens, F. J. Devlin, C. F. Chabalowski and M. J. J. Frisch, *J. Phys. Chem.*, 1994, **98**, 11623–11627.

26 L. Fabbrizzi, M. Licchelli, P. Pallavicini, A. Perotti and D. Sacchi, *Angew. Chem., Int. Ed.*, 1994, **33**, 1975–1977.